Table II. Standards Put Through Total Chemical and Mass Spectrometric Procedure

	mol %			
	234	235	236	238
av of 3, double plate	0.0657	10.0000	0.0373	89.8271
± std dev	0.0003	0.0019	0.0005	0.0021
av of 3, fumed	0.0664	10.0726	0.0377	89.8233
± std dev	0.0008	0.0020	0.0002	0.0024
NBS Cert.	0.0666	10.075	0.0376	89.821
± $t\sigma$	0.0002	0.010	0.0001	0.010

Table III. Component Procedure Blanks

process	amt, pg	mol % 234	235	236	238
electrodep chem	13.2		0.965		99.035
chem + fume	341		1.05	0.06	98.89
chem + plate	396	0.04	2.08	0.05	97.83
filament electrodep	0.1		6 ± 5		94 ± 5

the filament. Additional analyses were performed on samples from 1 to 30 ng with similar analytical characteristics. Filament fractionation appears constant from 5 to 15 ng. Outside this span some change occurs. Ten nanograms was chosen to limit loading blank contribution to less than 1×10^{-4}.

When measuring ratios which differ from unity, dead time corrections in pulse counting systems become very important. Figure 3 shows dead time corrections for a 10/1 ratio for various dead times. The dead time of our measuring system is determined by a pulse generator using pulsed pairs. It is independently checked by using NBS U-100 and NBS U-900, certified uranium isotopic standards with 235/238 ratios of ~1/10 and ~10/1, respectively. The standards were each analyzed five times, Table I. By use of the previous analyses of the NBS U-500 as a basis of determining the fractionation correction, it can be seen that good agreement with the certified values is achieved. The minor isotopes on these analyses demonstrate accuracies of 0.5% on ratios as small as 4×10^{-4}.

The above data demonstrate the capabilities of the mass spectrometric method alone. In the real world the samples are separated from rock and various other complex matrices. In order to check the total system, we put NBS U-100 through the total chemistry with three samples each electroplated and fumed, Table II. Parallel blanks were determined by using 99.9+% enriched ^{233}U. Total system blanks were less than 400 pg while the plating blank for putting the sample onto the anode was ~13 pg, and onto the filament ~0.1 pg. Table III shows these data. Agreement is good except for the case of ^{234}U in the double plating. The 6×10^{-4} ratio is measured with a negative bias of ~1%. The cause of this bias is unknown. Attempts to reduce system blank are being made to help eliminate these kinds of bias.

ACKNOWLEDGMENT

The authors thank A. J. Gancarz and D. B. Curtis for extensive chemical and critical support and Glen E. Bentley for the plasma emission spectrometer measurements.

LITERATURE CITED

(1) Rec, John R. Doctoral Thesis, Rennselaer Polytechnic Institute, Troy, NY, 1969.
(2) NBS Technical Note #426, Shields, William R., Ed. *NBS Tech. Note (U.S.)* **1967**, *No. 426*.
(3) Shideler, R. W. *Int. J. Mass Spectrom. Ion Phys.* **1976**, *21*, 213-219.

RECEIVED for review November 6, 1981. Accepted January 25, 1982.

Secondary Ion Mass Spectrometry of Protected Diribonucleoside Monophosphates with a Time-of-Flight Mass Spectrometer

Werner Ens and Kenneth G. Standing*

Department of Physics, University of Manitoba, Winnipeg, Manitoba, Canada R3T 2N2

John B. Westmore*

Department of Chemistry, University of Manitoba, Winnipeg, Manitoba, Canada R3T 2N2

Kelvin K. Ogilvie and Mona J. Nemer

Department of Chemistry, McGill University, Montreal, Quebec, Canada H3A 2K6

Positive and negative secondary ion mass spectra have been measured for eight fully protected diribonucleoside monophosphates with various permutations of bases and protecting groups. The spectra, produced by 8–28 keV Cs^+ ions, were examined in a time-of-flight mass spectrometer. The spectra yield a wealth of diagnostically useful information enabling determination of the molecular weight, identification of the protecting groups present, identification of the nucleobases present, and determination of the base sequence. Many of the ions are metastable (lifetimes ~10 μs or less). Preliminary studies on a protected triribonucleoside diphosphate confirm that the technique can be extended to molecules with molecular mass up to at least 2100.

Synthetic oligonucleotides have played a significant role in our understanding of many current problems in molecular biology. For the efficient synthesis of such nucleotide chains, it is necessary to protect the sensitive positions in the constituent nucleotides with appropriate blocking groups (*1*). During synthesis, it is important to verify the structure of the growing oligonucleotide and the final product. However, the well-developed methods for sequencing unprotected DNA (*2–4*) and RNA (*5*, *6*) segments are not applicable to the protected oligonucleotides since the presence of the protecting groups renders the molecule resistant to the normal sequencing enzymes or chemical reagents. Thus, it has normally been necessary to remove the protecting groups completely and then

0003-2700/82/0354-0960$01.25/0

Table I. Diribonucleoside Monophosphates Studied

	compound							
	1	2	3	4	5	6	7	8
B′	A	U	A	U	U	A^{Bz}	A^{Bz}	A
B″	U	U	U	U	U	U	U	U
R′	Sil	Sil	Sil	MMT	MMT	H	MMT	Sil
R″	Sil	Sil	Sil	Lv	Sil	Sil	Sil	Sil
X	O	O	S	O	O	O	O	absent

to analyze the deprotected nucleotide by the standard methods. Such procedures are time-consuming and involve relatively large amounts (50–100 mg) of the protected oligomer.

Mass spectrometry has been used extensively to characterize the constituent nucleosides of nucleic acids (*7*). However, the presence of the phosphate group makes the free nucleotides insufficiently volatile for conventional electron impact and chemical ionization techniques, so derivatization is necessary. This severely limits the application of these methods in larger oligonucleotides. Pyrolysis mass spectrometry breaks up the oligomers into relatively small fragments, so it yields little structural information (*8–10*).

The newer "soft ionization" techniques have been more successful. Field desorption has produced informative spectra from mononucleotides and from a number of dinucleoside monophosphates (*11*). Spectra for related compounds have also been reported for laser desorption mass spectrometry (*12, 13*). However, the most extensive measurements to date have been obtained by bombardment of the samples with ^{252}Cf fission fragments; protected nucleotide chains containing up to seven nucleosides have been studied (*14–18*) and ions of masses up to $m/z > 12500$ observed (*19*). More recently, mass spectra from mono- and dinucleotides have been produced by the impact of low-energy (keV) ions (*20–23*) and of low-energy neutral atoms (*24*) (molecular SIMS and fast atom bombardment [FAB], respectively); an $(M - H)^-$ ion from a tetranucleoside triphosphate has also been observed at m/z 1172 using the latter technique (*25*).

As mentioned above, analysis of *protected* oligonucleotides is of particular interest because of the failure of conventional methods. The presence of the protecting groups might be expected to increase the sample volatility; on the other hand, it gives a considerable increase in molecular mass. Pyrolysis mass spectrometry has in fact been applied to some of these compounds, but it has yielded little structural information, because of extensive fragmentation (*26, 27*). However, the results of McNeal and Macfarlane (*14–19*) mentioned above, and recent field desorption measurements (*28*), show that these compounds can be analyzed by mass spectrometry, using appropriate techniques.

The similarity between the mass spectra produced by low energy ion bombardment and by fission fragments (*22, 23*) suggests that protected nucleotides might also be analyzed by the impact of low-energy ions. Thus, we here describe the secondary ion mass spectra of some fully protected oligonucleotides, produced by bombardment with ~10 keV Cs^+ ions, and measured on the Manitoba time-of-flight mass spectrometer (*21*). In order to understand the basis of the fragmentations, we have chosen to study a limited class of such compounds in some detail, namely, the diribonucleoside monophosphates with uracil and adenine bases. Eight such compounds have been examined; these incorporate various permutations of nucleobases and protecting groups. Characteristic ion types which yield sequence information are also observed in the positive and negative secondary ion mass spectra of a protected triribonucleoside diphosphate.

EXPERIMENTAL SECTION

Protected di- and triribonucleoside phosphates were prepared at McGill University by the phosphite triester method (*1*). A few tens of nanomoles of each sample were electrosprayed (*29*) from methanol or acetone (without any other additions) to give a thin film on 2–3 cm^2 of the metal surface of aluminized polyester film. This is similar to the sample preparation technique used in the fission fragment measurements (*14–19*), but quite different from the method (solution or suspension in glycerol) applied in fast atom bombardment (*25*).

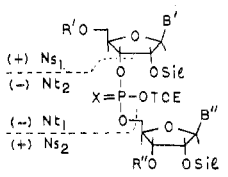

Figure 1. General structure of the protected diribonucleoside monophosphates: B′ = U, A, or A^{Bz}; B″ = U; R′ = H, Sil, or MMT; R″ = Lv or Sil; TCE = CCl_3CH_2; Sil = *t*-$BuMe_2Si$; Bz = C_6H_5CO; Lv = $CH_3COCH_2CH_2CO$; MMT = $CH_3OC_6H_4(C_6H_5)_2C$; X = O, S, or absent.

The target film was bombarded by a pulsed beam of Cs^+ ions at energies of 8–28 keV (~10 ns pulses at regular intervals of 200 μs). These struck the target at an angle of incidence of ~20°, i.e., 20° from the target normal, or 70° from the plane of the target. The *average* primary ion current was 0.1–1 pA, corresponding to an average current density ~3 to 30 pA/cm^2 on the 2 mm diameter beam spot. Again, these are rather different conditions from those which have typically been used in fast atom bombardment (2–8 keV Ar atoms at an angle of incidence of 70°, i.e., 20° from the plane of the target (*30*); particle flux equivalent to a current density ~1 to 10 nA/cm^2 (*24*) or a total beam current up to ~400 μA (*31*)).

The secondary ions produced in the target by Cs^+ ion bombardment were observed in the Manitoba time-of-flight mass spectrometer (*21*). In its present configuration this instrument has unit resolution up to $m/z \sim 1000$ in a favorable case (small initial energy spread). However, the observed peaks are normally broader than the time-resolving capabilities of the instrument (*21*). This characteristic peak broadening in time-of-flight spectrometers arises largely from detection of the decay products of the metastable decompositions which occur in the flight tube between the accelerating grid and the detector (*32*). The neutral or charged daughters are observed at the approximate position of the parent ion, but the peak is broadened because of the kinetic energy released in the decomposition. For an ion of $m/z \sim 1200$, the acceleration time is ~100 ns and the flight time is ~40 μs, so the broadening will be important for ion species with lifetimes in this range. A set of deflection plates 50 cm along the flight tube from the target enables all charged species to be deflected away from the detector so that neutral decomposition products from the metastable ions can be recorded (*21*).

When each individual secondary ion is detected, its time-of-flight is digitized and recorded in the memory of a multichannel analyzer. This memory is divided into a number of bins or channels (here 4000), each one corresponding to a given range of flight times (e.g., 20 010–20 020 ns). When the flight time of a secondary ion lies within a given channel, the number of counts in that memory bin is incremented by one. Thus the final time-of-flight spectrum (distribution of counts in the memory bins) represents the *integral* of the number of secondary ions ejected during the whole measurement.

Centroids of the broadened peaks are calculated by a program stored in the analyzer; the error in this computation is estimated to be ±1 at $m/z \sim 1000$. Above m/z 200 the experimental m/z values are given to the nearest integer. Calculated m/z values use chemical atomic masses so as to correspond to the isotopic averaging in the experimental centroids.

RESULTS AND DISCUSSION

The general composition of the protected diribonucleoside monophosphates examined is shown in Figure 1, while the specific compounds are listed in Table I. The complete positive and negative ion mass spectra of fully protected ApU, chosen to be representative of the compounds studied, are given in Figure 2. It can be seen that ions characteristic of

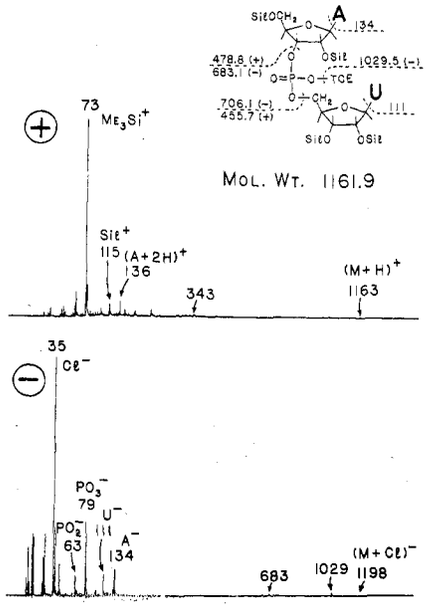

Figure 2. Positive and negative ion spectra of protected ApU (compound **1**): primary ions, 8 keV Cs^+ for positive spectrum, 28 keV Cs^+ for negative spectrum; duration of measurements, 20 min for positive spectrum, 10 min for negative spectrum.

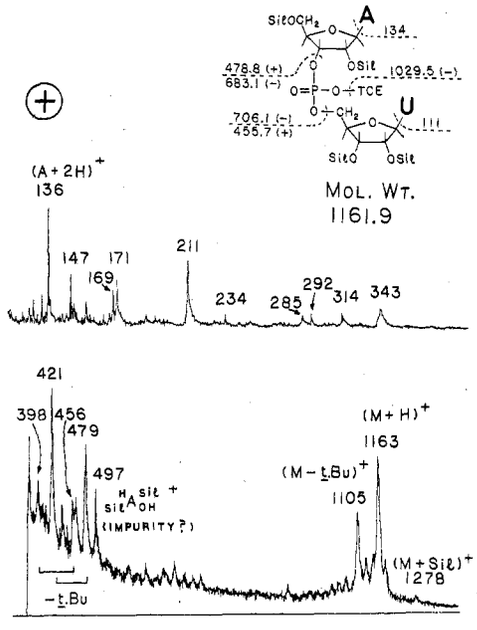

Figure 3. Positive ion spectra of protected ApU (compound **1**): (upper) expansion of region of Figure 2 between m/z 100 and 400, (lower) spectrum above m/z 400 after a fixed delay is introduced between the primary pulse and the start signal; primary ions, 8 keV Cs^+; duration of measurements, 20 min for upper spectrum, 35 min for lower spectrum.

the intact molecule represent only a small fraction of the total ions detected. The higher mass regions of both spectra are more readily observed in Figures 3 and 4. The upper part of Figure 3 is an expansion of the region of Figure 2 between m/z 100 and 400. The lower part is the spectrum above m/z 400 when a fixed delay is introduced between the primary pulse and the start signal (*21*). This delay prevents loss of counts in the high mass region from the abundant low mass ions. (In its present configuration our instrument uses single stop counting. This would result in a significant loss of signal for high mass ions, particularly if their emission from the sample surface is strongly correlated with the emission of low mass ions.) Similarly, the upper part of Figure 4 is an expansion of the negative ion spectrum of Figure 2 up to m/z

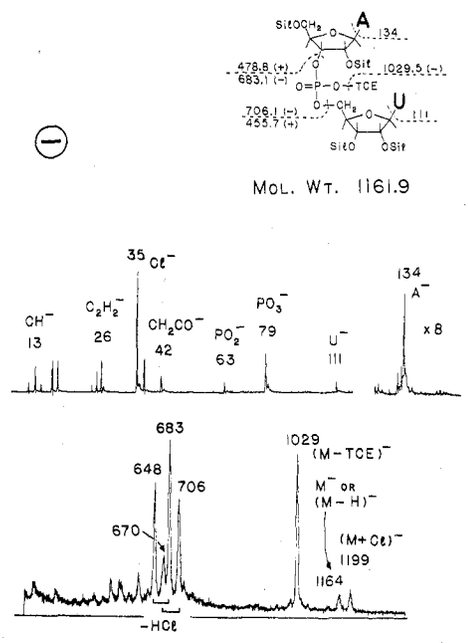

Figure 4. Negative ion spectrum of protected ApU (compound **1**): (upper) expansion of region of Figure 2 up to m/z 400, (lower) spectrum above m/z 400 after fixed delay; primary ions, 28 keV Cs^+; duration of measurements, 10 min for upper spectrum, 50 min for lower spectrum.

400. The lower portion is the spectrum above m/z 400 obtained after a fixed delay.

General Features of the Mass Spectra. The spectra, presented in Tables II and III, contain a wealth of diagnostically useful information for characterization of the molecule. The low mass regions yield prominent ions indicative of the protecting groups and nucelobases present. The silyl group is recognized by ions at m/z 115 and 73 in the positive ion spectrum, corresponding to t-$BuMe_2Si^+$ and its decomposition product Me_3Si^+, respectively. Ions indicative of uracil are observed at m/z 169, $[U + SiMe_2]^+$, in the positive ion spectrum, and at 111, $[U]^-$, in the negative ion spectrum. Similarly, adenine is recognized by m/z 136, $[A + 2H]^+$, in the positive ion spectrum, and by 134, $[A]^-$, in the negative ion spectrum. These assignments are consistent with intensity variations observed in electron impact positive ion mass spectra of ribonucleosides containing t-$BuMe_2Si$ protecting groups, where the peak for $[B + SiMe_2]^+$ is intense for pyrimidine nucleosides (frequently the base peak) and of low intensity for purine nucleosides (*33*). Conversely, the peak for $[B + 2H]^+$ is more intense for purine than for pyrimidine nucleosides. Molecules which contain the monomethoxytrityl group are easily recognized, not only by the prominent ion MMT^+ at m/z 273 but also by *net* losses of MMTO, CH_3O-C_6H_4, or C_6H_5 from the molecular ion.

Ions characteristic of the intact molecule enable the molecular weight to be determined. In the positive ion spectrum these arise by protonation, or through cationization by adventitious sodium ions, to give $[M + H]^+$ and $[M + Na]^+$. (Addition of other alkali metal ions, such as K^+, is also observed. When levels of Na^+ are relatively high, replacement of H by Na is observed to give species such as $[M - H + 2Na]^+$.) In the negative ion spectrum ions formed by proton loss, $[M - H]^-$, and chloride ion addition, $[M + Cl]^-$, are observed.

Positive Ions. Several positive fragment ions enable the components of the protected diribonucleoside monophosphates to be confirmed. In particular, cleavages of the O–C(3′) and O–C(5′) bonds yield the fragments designated as Ns_1^+ and Ns_2^+, respectively (see Figure 1). From these, in turn, daughter ions corresponding to losses of HB′ and HB″,

Table II. Positive Ion Correlation Table for Diribonucleoside Monophosphates

compound[a]									
1	2	3	4	5	6	7	8	assignment	*m/z* calcd
73	73	73	73	73	73	73	73	Me_3Si^+	73
75	75	75	75	75	75	75	75	Me_2SiOH^+	75
			99					Lv^+	99
					105	105		Bz^+	105
113	113	113	113	113	113	113	113	$[U + 2H]^+$	113
115	115	115	115	115	115	115	115	Sil^+	115
136		136			136	136	136	$[A + 2H]^+$	136
147	147	147		147	147	147		$Me_3SiOSiMe_2^+$	147
155	155	155		155	154	155		$UC_2H_4O^+$	155
170	169	169	169	169	169	169	169	$[U + SiMe_2]^+$	169
171	171	171		171	171	171	171		
211	211	211	211	211	211	211	211	$C_5H_4O_2Sil^+$ and $UC_2H_2OSiMe_2^+$	211
234		234			234	[ ]	234	$AC_2H_2OSiMe_2^+$	234
					240	240		$[A^{Bz} + 2H]^+$	240
			273	273		273		MMT^+	273
292	[ ]	292	[ ]	[ ]	292	[ ]	293		
285	285	285	[ ]	[ ]	171		285	$[Ns_1 - HB' - H - t\text{-Bu}]^+$	
(285.5)	(285.5)	(285.5)	(443.6)	(443.6)	(171.3)	(443.6)	(285.5)		
344	344	344	~500	499	229	499	344	$[Ns_1 - HB']^+$	
(343.6)	(343.6)	(343.6)	(501.7)	(501.7)	(229.4)	(501.7)	(343.6)		
421	398	421	558	556	412	683	421	$[Ns_1 - H - t\text{-Bu}]^+$	
(420.7)	(397.6)	(420.7)	(555.7)	(555.7)	(410.5)	(682.8)	(420.7)		
479	456	478	614	614	[ ]	[ ]	479	Ns_1^+	
(478.8)	(455.7)	(478.8)	(613.8)	(613.8)	(468.6)	(741.0)	(478.8)		
285	285	285	[ ]	286	285	285	285	$[Ns_2 - HB'' - H - t\text{-Bu}]^+$	
(285.5)	(285.5)	(285.5)	(269.4)	(285.5)	(285.5)	(285.5)	(285.5)		
344	344	344	326	343	343	343	344	$[Ns_2 - HB'']^+$	
(343.6)	(343.6)	(343.6)	(327.5)	(343.6)	(343.6)	(343.6)	(343.6)		
398	398	398	381	398	397	396	398	$[Ns_2 - H - t\text{-Bu}]^+$	
(397.6)	(397.6)	(397.6)	(381.5)	(397.6)	(397.6)	(397.6)	(397.6)		
456	456	456	440	456	456	456	456	Ns_2^+	
(455.7)	(455.7)	(455.7)	(439.6)	(455.7)	(455.7)	(455.7)	(455.7)		
			991	1007				$[M - MMTO]^+$	
			(991.4)	(1007.5)					
			1171	1188				$[M - CH_3OC_6H_4]^+$	
			(1173.6)	(1189.8)					
			1203	1219				$[M - C_6H_5]^+$	
			(1203.6)	(1219.8)					
			1181					$[M - Lv]^+$	
			(1181.6)						
[ ]	1029		1171	1188	[ ]	[ ]	1015	$[M - B']^+$	
(1027.7)	(1027.7)	(1043.8)	(1169.7)	(1185.8)	(913.5)	(1185.8)	(1011.7)		
1052	1029	1068	1171	1188	[ ]	[ ]	1035	$[M - B'']^+$	
(1050.8)	(1027.7)	(1066.8)	(1169.7)	(1185.8)	(1040.6)	(1313.0)	(1034.8)		
1105	1082	1121	1224	1240	1094	1368	1089	$[M - t\text{-Bu}]^+$	
(1104.7)	(1081.7)	(1120.8)	(1223.6)	(1239.8)	(1094.6)	(1366.9)	(1088.7)		
[ ]	1124	1163	1264	1283	[ ]	[ ]	1129	$[M - CH_3]^+$	
(1146.8)	(1123.8)	(1162.9)	(1265.7)	(1281.9)	(1136.7)	(1409.0)	(1130.8)		
1163	1140	1179	1281	1297	1152	1425	1147	$[M + H]^+$	
(1162.9)	(1139.8)	(1178.9)	(1281.7)	(1297.9)	(1152.7)	(1425.1)	(1146.9)		
1185	1162	1201	1304	1320	1175	1447	1169	$[M + Na]^+$	
(1185.8)	(1161.8)	(1200.9)	(1303.7)	(1319.9)	(1174.7)	(1447.0)	(1168.8)		
[ ]	[ ]	[ ]	[ ]	1335	[ ]	[ ]	1187	$[M + K]^+$	
(1201.0)	(1177.9)	(1217.0)	(1319.8)	(1136.0)	(1190.8)	(1463.1)	(1185.0)		
1278	1254	1295	[ ]	1413	[ ]	[ ]	1260	[M+ Sil]$^+$	
(1277.1)	(1254.1)	(1293.2)	(1396.0)	(1412.2)	(1267.0)	(1539.3)	(1261.1)		
					Other Ions				
					364	[ ]		$[Ns_1 + H - Bz]^+$	
					(364.5)	(636.8)			
					937	[ ]		$[M + H - Bz - B'']^+$	
					(936.5)	(1208.9)			
					990	1264		$[M + H - Bz - t\text{-Bu}]^+$	
					(990.5)	(1262.8)			
					1032	[ ]		$[M + H - Bz - CH_3]^+$	
					(1032.6)	(1304.9)			
					1048	1321		$[M + H - Bz + H]^+$	
					(1048.6)	(1320.9)			
						1343		$[M + H - Bz + Na]^+$	1342.9
915								$[M - B' - HB'']^+$	915.6
		1143					1112	$[M + Na - (H + t\text{-Bu})]^+$	
		(1142.8)					(1110.7)		

[a] Brackets denote ion type not observed significantly above neighboring background. Parentheses denote calculated values.

Table III. Negative Ion Correlation Table for Diribonucleoside Monophosphates

compound[a]									
1	2	3	4	5	6	7	8	assignment	*m/z* calcd
35/37	35/37	35/37	35/37	35/37	35/37	35/37	35/37	Cl^-	35/37
42	43?	42	42	42	42	42	42	CH_2CO^-	42
63	63	63	63	63	63	63	63	PO_2^-	63
79	79	79	79	79	79	79	79	PO_3^- (+POS^- for 3)	79
		95						PO_2S^-	95
111	111	111	111	111	111	111	111	U^-	111
			115					LvO^-	115
	131		~132		131	131		$SilO^-$	131
134		134			134	134	134	A^-	134
					238	238		A^{Bz-}	238
?	552	[ ]	[ ]	[ ]	[ ]	[ ]	559	$[Nt_1 + H - TCE]^-$	
(574.7)	(551.7)	(590.8)	(709.8)	(709.8)	(564.6)	(836.9)	(558.7)		
570	570	585	[ ]	[ ]	[ ]	[ ]	[ ]	$[Nt_1 - HB']^-$	
(571.0)	(571.0)	(587.1)	(729.1)	(729.1)	(456.7)	(729.1)	(578.0)		
670	648	686	805	806	[ ]	934	[ ]	$[Nt_1 - HCl]^-$	
(669.7)	(646.6)	(685.8)	(804.7)	(804.7)	(659.5)	(931.9)	(653.7)		
706	683	722	841	841	[ ]	969	[ ]	Nt_1^-	
(706.1)	(683.1)	(722.2)	(841.2)	(841.2)	(696.0)	(968.3)	(690.1)		
552	552	568	536	552	552	551	536	$[Nt_2 + H - TCE]^-$	
(551.7)	(551.7)	(567.8)	(535.5)	(551.7)	(551.7)	(551.7)	(535.7)		
570	570	585	555	571	570	569	[ ]	$[Nt_2 - HB'']^-$	
(571.0)	(571.0)	(587.1)	(554.8)	(571.0)	(571.0)	(571.0)	(555.0)		
648	648	664	630	647	648	648	632	$[Nt_2 - HCl]^-$	
(646.6)	(646.6)	(662.7)	(630.5)	(646.6)	(646.6)	(646.6)	(630.7)		
683	683	699	667	683	683	683	667	Nt_2^-	
(683.1)	(683.1)	(699.2)	(666.9)	(683.1)	(683.1)	(683.1)	(667.1)		
1029	1006	1045	1149	1164	1020	1292	1013	$[M - TCE]^-$	
(1029.5)	(1006.4)	(1045.5)	(1148.3)	(1164.5)	(1019.3)	(1291.6)	(1013.5)		
1161	1138	1178	1280	1297	1151	1425	1147	$[M - H]^-$	
(1160.8)	(1137.8)	(1176.9)	(1279.7)	(1295.9)	(1150.7)	(1423.0)	(1144.9)		
1198	1174	1215	1317	1333	1188	1460	1181	$[M + Cl]^-$	
(1197.3)	(1174.3)	(1213.3)	(1316.2)	(1332.4)	(1187.1)	(1459.5)	(1181.9)		
Other Ions									
			569					$[Nt_2 + H - Lv]^-$	568.8
			1050					$[M + H - Lv - TCE]^-$	1050.2
					990	1264		$[M + H - Bz - t\text{-Bu}]^-$	
					(990.5)	(1262.8)			
					1048	1321		$[M + H - Bz - H]^-$	
					(1046.6)	(1318.9)			
					1070	1341		$[M + Na - Bz - H]^-$	
					(1068.6)	(1340.9)			
				891				$[M + H - MMT - TCE]^-$	892.1
						1153		$[M + H - MMT - H]^-$	1150.7
						1176		$[M + Na - MMT - H]^-$	1172.7
					915			$[M + H - Bz - TCE]^-$	915.2
					1047			$[M + H - Bz - H]^-$	1046.6
					1084	1357		$[M + H - Bz + Cl]^-$	
					(1083.0)	(1355.4)			
						1019		$[M + H - MMT - TCE]^-$	1019.3
						1152		$[M + H - MMT - H]^-$	1150.7
						1188		$[M + H + Cl]^-$	1187.1
						1083		$[M + 2H - Bz - MMT + Cl]^-$	1083.0
							648	$[Nt_2 + O - HCl]^-$	648.7
							683	$[Nt_2 + O]^-$	683.1
							706	$[Nt_1 + O]^-$	706.1
							1029	$[M + O - TCE]^-$	1029.5

[a] Brackets denote ion type not observed significantly above neighboring background. Parentheses denote calculated values.

respectively, and of (t-Bu + H) are normally observed (see Table II). Structures a and b, proposed for the former pair, can be formed via favorable six-membered cyclic transition states involving transfer of H(2′) to the base, in a mechanism analogous to that observed in electron impact spectra of derivatized nucleosides (*33*).

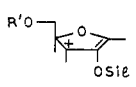

a, $[Ns_1 - HB']^+$

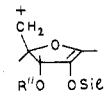

b, $[Ns_2 - HB'']^+$

Scheme I

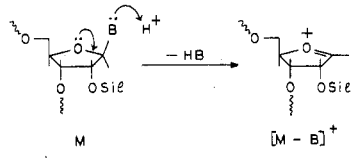

Fragment ions observed in the high mass region correspond to $[M - B']^+$, $[M - B'']^+$, $[M - t\text{-Bu}]^+$, and $[M - CH_3]^+$. Elimination of the nucleobases may be assisted by proton transfer from neighboring molecules at, or near, the surface

of the sample film, as shown in Scheme I. Analogues of $[M - B]^+$ are well-known in both electron impact and chemical ionization mass spectra of underivatized and derivatized nucleosides and nucleotides (*7*). Losses of *t*-Bu or CH_3 are most easily explained by siliconium ion formation as in conventional electron impact mass spectrometry.

The observation of the ion $[M + Sil]^+$ is of interest because the addition of a bulky Sil· or Sil^+ to $M^{+}\cdot$ or M, respectively, does not seem likely. It may correspond instead to a protonated molecule which contains an extra silyl protecting group (probably on the nucleobase, and of mass M – H + Sil).

The assignment of some ions in the positive ion spectra below *m/z* 300 is less straightforward A prominent ion at *m/z* 211 in all spectra has a counterpart at *m/z* 234 when adenine is also present in the molecule. This suggests an assignment of $[B + 100]^+$ for these ions, corresponding to the species $[BCH{=}CHOSiMe_2]^+$ observed in electron impact mass spectra of ribonucleosides having a 2′-O-*t*-$BuMe_2Si$ protecting group (*33*). However, not all (or even most) of the peak at *m/z* 211 can be assigned in this way because it is also prominent in ^{252}Cf plasma desorption mass spectra of protected oligoribonucleotides which do not contain uridine (*18*). This ion lacks the isotopic pattern of Cl and is prominent when the MMT group is absent. A stable ion, totally consistent with these observations, is $[C_5H_4O_2Sil]^+$, structure c, possibly having aromatic stabilization, structure d. An ion of this type has

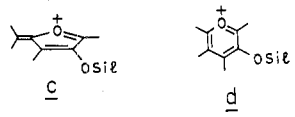

c d

been characterized in the electron impact mass spectra of *t*-$BuMe_2Si$ derivatives of ribonucleosides (*33*). This ion type is also well-known in the electron impact mass spectra of other derivatized nucleosides and nucleotides and is the base peak in many spectra (*7*). Its formation requires at least two hydrogen rearrangements, processes which are characteristically slower than simple bond fissions. Significantly, while many of the peaks in the spectra show symmetrical broadening from metastable decompositions in the field free flight tube (see below) the peak at *m/z* 211 shows marked asymmetry (high time tail) which is typical of decomposition in the acceleration region, but near the sample surface (*32*), involving decompositions in a time window extending to about 10 ns after initial impact of the primary particle, for the conditions prevailing in our instrument.

A peak at *m/z* 155, present in most positive ion spectra (see Table II), has a counterpart at *m/z* 178 in the ^{252}Cf plasma desorption mass spectra of protected oligonucleotides having adenosine as the 3′-terminal nucleoside (*18*). It can therefore be assigned as $[B + 44]^+$, most likely as $HB^+CH{=}CHOH$.

Negative Ions. The negative ion spectra yield information complementary to that obtained from the positive ion spectra. In fact, the negative ion spectra are generally cleaner and easier to interpret, and specific bond cleavages seem to occur more reproducibly than in the positive ion spectra.

An important group of bond fissions leads to formation of dialkyl phosphate ions by cleavage of O–C bonds to give the ions designated as Nt_1^- and Nt_2^- (see Figure 1) which are the fragments complementary to Ns_2^+ and Ns_1^+, respectively, and also $[M - TCE]^-$. Daughter ions from the two Nt^- species are $[Nt - HCl]^-$ or, alternatively, $[Nt - Cl]^-$ (both within our uncertainty limits), $[Nt - HB]^-$, and $[Nt + H - TCE]^-$. The formation of $[Nt - HB]^-$ could occur by a mechanism involving loss of H(2′), similar to that proposed above for formation of $[Ns - HB]^+$, while formation of $[Nt + H - TCE]^-$ can be rationalized by replacement of the TCE group by H, possibly from a neighboring molecule at or near the surface of the sample film (Scheme II).

Scheme II

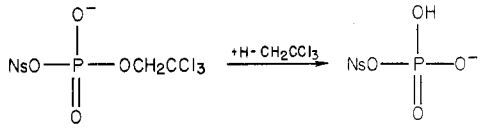

$[Nt_{1\text{ or }2} + H - TCE]^-$

Other Features of the Mass Spectra. The secondary ion mass spectra are sensitive to certain types of impurity. In general, it is not possible to estimate the concentration of the impurities in the bulk sample since they may be concentrated at the very surface of the sample film. Ions which have been recognized as arising from impurities have been listed in the lower parts of Tables II and III.

The positive and negative ion spectra of compounds **6** and **7**, which were electrosprayed from methanol, show clearly the presence of impurities in which the adenine base has been debenzoylated. (Studies of debenzoylation of *N*-benzoylribonucleosides having a *t*-$BuMe_2Si$ group at O(5′) and/or O(2′) have shown (*34*) the relative rates of debenzoylation to be *N*-benzoylcytidines > *N*-benzoyladenosines > *N*-benzoylguanosines.) These impurities (in which H replaces Bz) give rise to ions appearing 104 below those corresponding to benzoylated species. In a similar way, other spectra show evidence for impurities formed by replacement of levulinyl or monomethoxytrityl substituents with hydrogen, or sometimes by silyl. An impurity arising from a different cause is observed in the positive and negative ion spectra of compound **8** where some oxidation of the phosphite linkage to give phosphate has occurred, producing a mass increase of 16 in ions which contain this grouping. Interestingly, while $[M + H]^+$ and $[M + Na]^+$ ions arising from such oxidation are not prominent, fragment ions, such as $[Nt + O]^-$ are much more so.

While it is probable that the impurities could be eliminated by repurifying the samples or electrospraying from a different solvent, these observations emphasize the usefulness of our technique for detecting them.

Metastable Ions. A large fraction of the ions produced from large molecules by fission fragment or kiloelectronvolt ion bombardment are found to be metastable (*21–23*, *32*). As pointed out in the Experimental Section, a set of deflection plates about one-third of the way along the flight tube may be used to deflect all charged particles out of the counter. Under these conditions only neutral particles resulting from metastable decompositions between the target and the deflecting plates are detected, i.e., from decompositions of parent ions within ~10 μs after their production. The neutral daughters are recorded at the approximate position of the parent ion.

Typical time-of-flight spectra of neutral fragments from compound **1** are shown in Figure 5. The vertical scales in these spectra are the same as those in the lower parts of Figures 3 and 4 so that it is possible to estimate directly the fraction of each ion type which decomposes. For example, from relative peak heights we estimate that ~40% of $[M + H]^+$ ions decompose within ~10 μs. Differences in ion lifetime are more pronounced for the cluster of ions 648 to 706 in the spectrum of neutrals from negative ions where the approximate percentages of ions which decompose are 648 (60%), 670 (100%), 683 (30%), and 706 (60%).

Other Studies. The techniques described are being extended to heavier molecules. As an example, Figure 6 shows the positive and negative secondary ion spectra of fully protected CpApU. The fragmentation pattern may be easily understood in terms of processes observed for the diribonucleoside monophosphates. The major cleavages take place at the internucleotide C–O bonds as before, resulting in for-

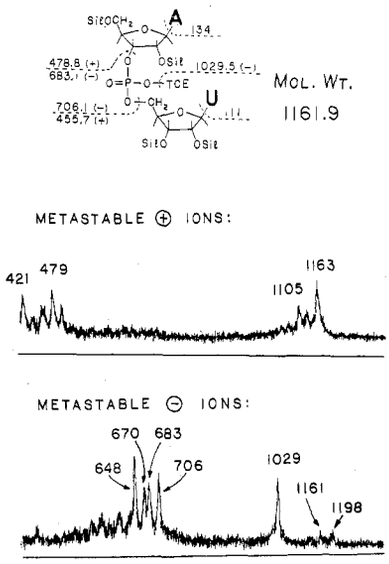

Figure 5. Time-of-flight spectra of neutral products from decomposition of metastable ions (i.e., ions which decompose between the acceleration grid and the deflecting plates). The vertical scales are the same as those in the lower parts of Figures 3 and 4.

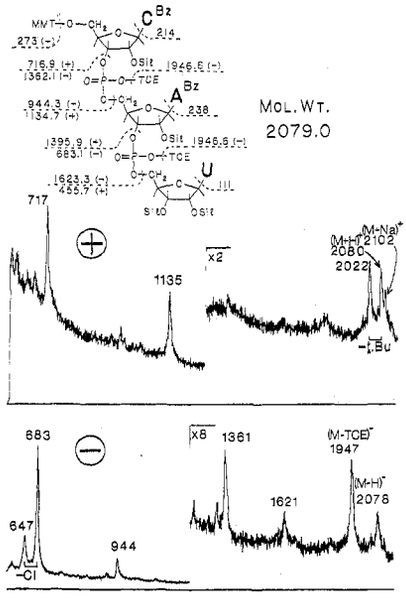

Figure 6. Positive and negative ion spectra of protected CpApU: primary ions, 10 keV Cs^+ for positive spectrum, 26 keV Cs^+ for negative spectrum; duration of measurements, 120 min for positive spectrum, 60 min for negative spectrum.

mation of positive carbonium ions and negative phosphate ions, as can also be seen from Figure 6.

Comparison with Other Techniques. The spectra of protected nucleotides reported here are very similar to those obtained by fission fragment bombardment (*14–19*), consistent with the results observed for other involatile compounds in this mass range (*22, 23*). As yet there have been no spectra of protected nucleotides reported for fast atom bombardment. However, judging from the similar fragmentation observed for unprotected nucleotides (*20–25*) and for peptides (*24, 35*) and from the probable common mechanism of the two processes (*36*), we should expect results similar to ours to be obtainable with this technique. Likewise, no protected nucleotides have been examined by laser desorption, but the similarity of the spectra of unprotected nucleotides observed for this method and for fission fragment bombardment (*13*) would argue that similar spectra might again be obtained for this technique. In the case of field desorption only the positive ion spectra of protected deoxyribonucleotides and dinucleotides have been reported (*28*). These spectra are considerably simpler than those obtained by energetic particle bombardment and consist primarily of protonated and cationized species characteristic of the intact molecule, with a small number of fragment species.

ACKNOWLEDGMENT

We thank R. Beavis for his assistance with the measurements, R. D. Macfarlane and C. J. McNeal for helpful discussions and ideas, for preprints, and for access to unpublished ^{252}Cf plasma desorption mass spectra of protected oligonucleotides, and F. H. Field and B. T. Chait for preprints.

LITERATURE CITED

(1) Ogilvie, K. K.; Nemer, M. J. *Can. J. Chem.* **1980**, *58*, 1389–1397 and references therein.
(2) Sanger, F.; Coulson, A. R. *J. Mol. Biol.* **1975**, *94*, 441–448.
(3) Maxam, A. M.; Gilbert, W. *Proc. Natl. Acad. Sci. U.S.A.* **1977**, *74*, 560–564.
(4) Tu, C. D.;Jay, E.; Bahl, C. P.; Wu, R. *Anal. Biochem.* **1976**, *74*, 73–93.
(5) Simoncsits, A.; Brownlee, G. G.; Brown, R. S.; Rubin, J. R.; Guilley, H. *Nature (London)* **1976**, *269*, 833–836.
(6) Gupta, R. G.; Randerath, K. *Nucleic Acid Res.* **1977**, *4*, 3441–3454.
(7) Hignite, C. In "Biochemical Applications of Mass Spectrometry"; Waller, G. R., Dermer, O. C., Eds.; Wiley-Interscience: New York, 1980; First Supplementary Volume, Chapter 16, pp 527–566.
(8) Schulten, H.-R.; Beckey, H. D.; Boerboom, A. J. H.; Meuzelaar, H. L. C. *Anal. Chem.* **1973**, *45*, 2358–2362.
(9) Wiebers, J. L. *Nucleic Acid Res.* **1976**, *3*, 2959–2970.
(10) Wiebers, J. L.; Shapiro, J. A. *Biochemistry* **1977**, *16*, 1044–1050.
(11) Schulten, H.-R. *Int. J. Mass Spectrom. Ion Phys.* **1979**, *32*, 97–283 and references therein.
(12) Posthumus, M. A.; Kistemaker, P. G.; Meuzelaar, H. L. C.; Ten Noever de Brauw, M. C. *Anal. Chem.* **1978**, *50*, 985–991.
(13) Schueler, B.; Krueger, F. R. *Org. Mass Spectrom.* **1980**, *15*, 295–301.
(14) McNeal, C. J.; Narang, S. A.; Macfarlane, R. D.; Hsiung, H. M.; Brousseau, R. *Proc. Natl. Acad. Sci. U.S.A.* **1980**, *77*, 735–739.
(15) McNeal, C. J. Ph.D. Dissertation, Texas A & M University, 1980, University Microfilms, Ann Arbor, MI.
(16) McNeal, C. J.; Ogilvie, K. K.; Theriault, N. Y.; Nemer, M. J. *J. Am. Chem. Soc.* **1982**, *104*, 972–975.
(17) McNeal, C. J.; Ogilvie, K. K.; Theriault, N. Y.; Nemer, M. J. *J. Am. Chem. Soc.* **1982**, *104*, 976–980.
(18) McNeal, C. J.; Ogilvie, K. K.; Theriault, N. Y.; Nemer, M. J. *J. Am. Chem. Soc.* **1982**, *104*, 981–984.
(19) McNeal, C. J.; Macfarlane, R. D. *J. Am. Chem. Soc.* **1981**, *103*, 1609–1610.
(20) Eicke, A.; Sichtermann, W.; Benninghoven, A. *Org. Mass Spectrom.* **1980**, *15*, 289–294.
(21) Chait, B. T.; Standing, K. G. *Int. J. Mass Spectrom. Ion Phys.* **1981**, *40*, 185–193.
(22) Standing, K. G.; Ens, W. E.; Chait, B. T.; Field, F. H. Proceedings of the International Conference on Ion Formation from Organic Solids, Münster, Germany, 6–8 Oct 1980; Springer Series in Chemical Physics, in press.
(23) Ens, W.; Standing, K. G.; Chait, B. T.; Field, F. H. *Anal. Chem.* **1981**, *53*, 1241–1244.
(24) Barber, M.; Bordoli, R. S.; Sedgwick, R. D.; Tyler, A. N. *Nature (London)* **1981**, *293*, 270–275.
(25) Williams, D. H.; Bradley, C.; Bojesen, G.; Santikarn, S.; Taylor, S. C. E. *J. Am. Chem. Soc.* **1981**, *103*, 5700–5704.
(26) Armbruster, M. A.; Wiebers, J. L. *Anal. Biochem.* **1977**, *83*, 570–579.
(27) Ulrich, J.; Bobenrieth, M. J.; Derbyshire, R.; Finas, F.; Guy, A.; Odin, F.; Polverelli, M.; Téoule, R. *Z. Naturforsch., B* **1980**, *35B*, 212–216.
(28) Schiebel, H. M.; Schulten, H.-R. *Z. Naturforsch., B* **1981**, *36B*, 967–973.
(29) McNeal, C. J.; Macfarlane, R. D.; Thurston, E. L. *Anal. Chem.* **1979**, *51*, 2036–2039.
(30) Barber, M.; Bordoli, R. S.; Sedgwick, R. D.; Tetler, L. W. *Org. Mass Spectrom.* **1981**, *16*, 256–260.
(31) Barber, M.; Bordoli, R. S.; Sedgwick, R. D.; Tyler, A. N. *Biomed. Mass Spectrom.* **1981**, *8*, 492–495.
(32) Chait, B. T.; Field, F. H. *Int. J. Mass Spectrom. Ion Phys.* **1981**, *41*, 17.
(33) Quilliam, M. A.; Ogilvie, K. K.; Sadana, K. L.; Westmore, J. B. *Org. Mass Spectrom.* **1980**, *15*, 207–219.
(34) Ogilvie, K. K.; Entwistle, D. W. *Carbohydrate Res.* **1981**, *89*, 203–210.
(35) Westmore, J. B.; Ens, W.; Standing, K. *Biomed. Mass Spectrom.*, in press.
(36) McNeal, C. J. *Anal. Chem.* **1982**, *54*, 43 A–50 A.

RECEIVED for review November 12, 1981. Accepted January 25, 1982. We thank the Natural Sciences and Engineering Research Council of Canada for financial support of this work and for award of a scholarship to W.E.